

# Carbonyl-Nitrido Mixed-Metal Clusters: Synthesis, Reactivity, Electrochemical Behavior and Solid-State Structure of $[\text{Co}_5\text{MoN}(\text{CO})_{14}]^{2-}$ and $[\text{Co}_5\text{MoN}(\text{CO})_{14}\text{AuPPh}_3]^-$

Roberto Della Pergola,<sup>\*,[a]</sup> Alessandro Fumagalli,<sup>[b]</sup> Fabrizia Fabrizi de Biani,<sup>[c]</sup> Luigi Garlaschelli,<sup>[d]</sup> Franco Laschi,<sup>[c]</sup> Maria Carlotta Malatesta,<sup>[d]</sup> Mario Manassero,<sup>\*,[e]</sup> Elena Roda,<sup>[d]</sup> Mirella Sansoni,<sup>[e]</sup> and Piero Zanello<sup>[c]</sup>

**Keywords:** Cobalt / Molybdenum / Cluster compounds / Nitrides / Electrochemistry

The dianionic cluster  $[\text{Co}_5\text{MoN}(\text{CO})_{14}]^{2-}$  (**1**) was synthesized from  $[\text{Co}_6\text{N}(\text{CO})_{15}]^-$  and  $[\text{Mo}_2(\text{CO})_{10}]^{2-}$  in refluxing acetonitrile. The solid-state structure of the  $[\text{Ph}_4\text{P}]^+$  salt was determined. It consists of an octahedral metal cage, enclosing a six-coordinate nitrido ligand. Typical bond lengths are: Co–N 1.88 Å, Mo–N 2.03 Å, Co–Co 2.61 Å and Co–Mo 2.84 Å, showing that there is very little, if any, preferential interaction of the interstitial atom with that of molybdenum. The cluster reacts with  $\text{Au}(\text{PPh}_3)\text{Cl}$  in THF at room temperature forming the derivative  $[\text{Co}_5\text{MoN}(\text{CO})_{14}\{\text{AuPPh}_3\}]^-$  (**2**). The gold atom caps an  $\text{MoCo}_2$  face of the octahedron, with short

Au–Co (2.68 Å) and long Au–Mo (3.16 Å) bonds, showing that both metal atoms are necessary for coordination, but  $\text{Au}^{\text{I}}$  binds better with the cobalt atoms. Electrochemical studies have pointed out that cluster **1** has good redox capabilities in that it is able to support reversibly the progressive addition of three electrons. EPR measurements on the corresponding trianion confirm the lack of preferential interaction between the Mo site and the interstitial nitride atom.

(© Wiley-VCH Verlag GmbH & Co. KGaA, 69451 Weinheim, Germany, 2004)

## Introduction

Recently, we described the synthesis and the chemical characterization of octahedral mixed-metal clusters of iron and a metal of group 6 (Mo or W), containing an interstitial nitride. Even if the yields were only just acceptable, they were obtained selectively, using different complexes with ligands of a different nature (CO, Cp, MeCN).<sup>[1]</sup> As an extension of this type of chemistry, we moved to the synthesis of Co–Mo nitrides. The choice of these two elements was based on the industrial relevance of Mo and Co

in hydrodesulfurization (HDS) and hydrodenitrogenation (HDN) reactions.<sup>[2]</sup> Molecular organometallic complexes have many applications in this field, since they contribute to clarifying the mechanism of the hydrogenation of thio and aza compounds.<sup>[3]</sup> In this context, clusters are especially of value, since they can homogeneously catalyze the hydrogenation of heterocycles<sup>[4]</sup> or model the interaction between N- and S-donors with multimetallic sites.<sup>[5]</sup> Even more important, sulfido Co–Mo clusters can stoichiometrically desulfurize thio compounds by a mechanism that is believed to closely mimic heterogeneous HDS.<sup>[6]</sup> Additionally, dimetallic sulfides can be prepared from a molecular precursor, either by supporting heterometallic Co–Mo clusters,<sup>[7]</sup> or by co-impregnation of homometallic carbonyl complexes.<sup>[8]</sup>

We started these investigations hoping that clusters containing Co, Mo and N could help us to understand the mutual relationships between the three elements. The first results of our efforts is the reproducible synthesis of a new cluster,  $[\text{Co}_5\text{MoN}(\text{CO})_{14}]^{2-}$ , which could be fully characterized through a combination of chemical, spectroscopic, electrochemical and X-ray analyses. The yields of the anion are moderate, but its preparation is much simpler than those reported for other Co–Mo nitride complexes,<sup>[9]</sup> mak-

[a] Dipartimento di Scienze dell'Ambiente e del Territorio, Università di Milano-Bicocca, Bicocca-piazza della Scienza 1, 20126 Milano, Italy  
E-mail: roberto.dellapergola@unimib.it

[b] Dipartimento di Biologia Strutturale e Funzionale, Università degli Studi dell'Insubria, Via J. H. Dunant 3, 21100 Varese, Italy

[c] Dipartimento di Chimica dell'Università di Siena, Via A. Moro, 53100 Siena, Italy

[d] Dipartimento di Chimica Inorganica, Metallorganica ed Analitica, Università di Milano, Via G. Venezian 21, 20133 Milano, Italy

[e] Dipartimento di Chimica Strutturale e Stereochimica Inorganica, Università di Milano, Via G. Venezian 21, 20133 Milano, Italy  
E-mail: m.manassero@csmtbo.mi.cnr.it

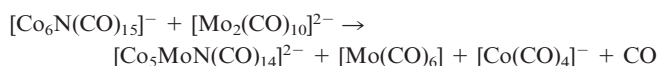
Supporting information for this article is available on the WWW under <http://www.eurjic.org> or from the author.

ing the cluster available on a decigram scale for further investigations.

## Results

### Synthesis and Reactivity

With the aim of synthesizing a nitrido Co–Mo cluster, we tried the same synthetic approach as was successfully used for the Fe–Mo analogs,<sup>[1]</sup> i.e. the condensation of a cobalt nitride, having a small negative charge, with a highly reduced carbonyl anion of molybdenum. Thus, the new product  $[\text{Co}_5\text{MoN}(\text{CO})_{14}]^{2-}$  (**1**) was obtained by reaction of  $[\text{Co}_6\text{N}(\text{CO})_{15}]^-$  ( $\text{K}^+$  salt) and  $[\text{Mo}_2(\text{CO})_{10}]^{2-}$  ( $\text{NEt}_4^+$  salt) in refluxing acetonitrile. IR monitoring shows that the reaction proceeds smoothly, the only by-products detectable in solution being the mononuclear carbonyl complexes  $[\text{Co}(\text{CO})_4]^-$  and  $[\text{Mo}(\text{CO})_6]$ .<sup>[10]</sup> However, a fairly large amount of decomposition product is formed, which can easily be eliminated by filtration. Dianion **1** can be purified by metathesis with  $[\text{Ph}_4\text{P}]^+$  in MeOH, which induces precipitation. We tested other less reducing complexes of molybdenum, such as  $[\text{Mo}(\text{CO})_3(\text{NCet})_3]$  or  $[\text{HMo}_2(\text{CO})_{10}]^-$ , but the resulting yields were even lower. Thus, the formation of **1** can be formally represented by the reaction



The reactivity of **1** with several potential sources of S- or N-ligands (such as quinoline,  $\text{NOBF}_4$ ,  $\text{Ph}_2\text{S}_2$ ) was examined. In order to perform ligand substitution, we attempted both the direct carbonyl displacement and “oxidative substitution”,<sup>[11]</sup> analogous with what has been used for other dianionic octahedral clusters.<sup>[12]</sup> Unfortunately, no stable derivatives were ever obtained. Attempts to add hydride ligands to **1** by protonation resulted in the formation of  $[\text{Co}_6\text{N}(\text{CO})_{15}]^-$ , in keeping with a weak interaction between the nitrogen and the molybdenum atom. All these disappointing results led us to further investigate the redox capability of **1**, thus prompting electrochemical investigations (see later). By contrast, the reaction between **1** and  $\text{Au}(\text{PPh}_3)\text{Cl}$  in THF at room temperature is fast and clean, quantitatively yielding  $[\text{Co}_5\text{MoN}(\text{CO})_{14}\{\text{AuPPh}_3\}]^-$  within a few minutes. The isolation of this adduct demonstrated that the poor reactivity of the dianion **1** cannot be attributed to the absence of nucleophilic character, nor steric crowding of its carbonyl ligands. Due to its composition of early-, late- and post-transition elements, the trimetallic  $[\text{Co}_5\text{MoN}(\text{CO})_{14}\{\text{AuPPh}_3\}]^-$  can be well classified among the “very-mixed”-metal carbonyl clusters.<sup>[13]</sup>

### The Solid-State Structures

The crystal structure of cluster **1** was determined on the  $[\text{Ph}_4\text{P}]_2\textbf{1}$  salt, and the geometry of the anion is shown in

Figure 1.<sup>[14]</sup> Average values of bond lengths are collected in Table 1, and compared with the corresponding parameters determined in **2**. The individual values are reported in Table S4 of the Supporting Information. The six metal atoms define an octahedron, centered by an interstitial nitride. As normally observed in Co clusters, the four unbridged edges are definitely longer than the bridged ones.<sup>[15]</sup> Examining the metal–metal and the metal–nitrogen bond lengths of other nitrido Co–Mo complexes,<sup>[9]</sup> Dahl discovered that Mo–N interactions are shorter than expected, and concluded that the Mo–N bond order was higher than the Co–N bond order. The same arguments were also used for nitrido Fe–Mo clusters,<sup>[1]</sup> with a strong interaction between the electron-deficient molybdenum atoms and the nitride (a well-known strong  $\pi$ -donor).<sup>[16]</sup> In the present case the uncertainty of the metallic radius of the cobalt atoms is high, since the Co–Co bond lengths are scattered by the

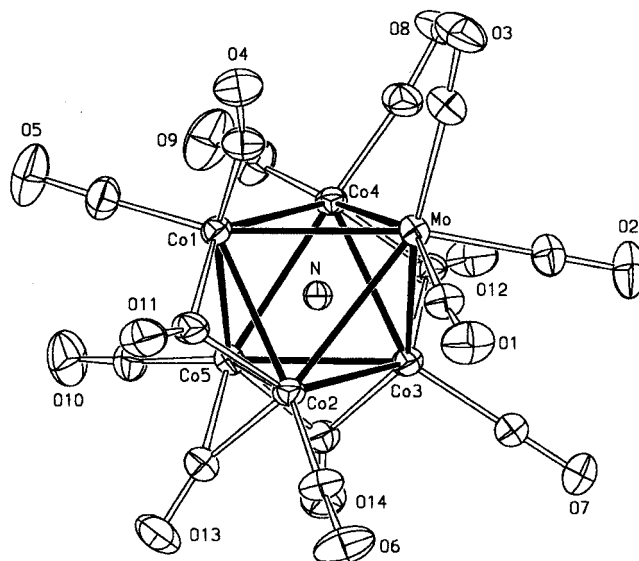


Figure 1. The solid-state structure of  $[\text{Co}_5\text{MoN}(\text{CO})_{14}]^{2-}$ ; carbon atoms are labeled using the oxygen atom to which they are attached

Table 1. Average interatomic distances [ $\text{\AA}$ ] in the clusters **1** and **2** (t = terminal, br = bridging); numbers in parentheses are esds on unique values,  $\pm$  numbers are rmsds on average bond lengths

	<b>1</b>	<b>2</b>
Co–Mo	$2.84 \pm 0.04$	$2.85 \pm 0.05$
Co–Co (unbridged)	$2.72 \pm 0.01$	$2.65 \pm 0.04$
Co–Co (bridged)	$2.50 \pm 0.07$	$2.531 \pm 0.004$
Au–Mo	–	3.159(1)
Au–Co	–	$2.68 \pm 0.07$
Au–P	–	2.312(1)
Mo–N	2.025(1)	2.061(1)
Co–N	$1.88 \pm 0.01$	$1.88 \pm 0.01$
Mo–CO <sub>t</sub>	$1.96 \pm 0.03$	$2.00 \pm 0.01$
Co–CO <sub>t</sub>	$1.76 \pm 0.01$	$1.77 \pm 0.02$
Co–CO <sub>br</sub>	1.94	1.96
C <sub>t</sub> –O <sub>t</sub>	1.15	1.15
C <sub>br</sub> –O <sub>br</sub>	1.16	1.17

presence of bridged and unbridged bonds (the root mean square deviations are listed in Table 1). The average values in **1** are  $2.61 \pm 0.12$  Å for the Co–Co distances and  $2.84 \pm 0.04$  Å for the Mo–Co bonds. Therefore the metallic radius of the Co atom can be estimated as being  $0.23 \pm 0.12$  Å smaller than that of Mo. On the other hand, the average Co–N bond is only  $0.15 \pm 0.01$  Å shorter than the Mo–N distance. The discrepancy between the two values (0.08 Å) is obviously smaller than the root mean square deviations and statistically uninformative. Nevertheless, with this difference being similar to that of other related clusters,<sup>[9]</sup> one would be tempted to presume that in **1** a small displacement of the nitride towards the Mo atom occurs.

The idealized symmetry of the whole anion is  $C_s$ , with the mirror plane passing through Mo, N and the midpoint of the Co2–Co3 edge. The cluster is surrounded by ten terminal and four edge-bridging carbonyl groups, distributed in such a way that all metal atoms are connected to three ligands. The Mo and Co atoms differ in the bonding mode of the ligands, due to their different valence electrons: Mo is connected to terminal ligands only, Co1 and Co4 to two terminal and one bridging group, Co2 and Co3 to one terminal and two bridging CO groups. With respect to this, it is remarkable that the dimetallic cluster **1** displays the same arrangement of bridging ligands found in  $[\text{Co}_6\text{N}(\text{CO})_{13}]^-$ , with four  $\mu$ -CO groups “spanning a sequence of four bonds”.<sup>[15]</sup> As a matter of fact the octahedral clusters of Rh and Co that contain an interstitial atoms and thirteen ligands, all adopt a different stereochemistry of the carbonyls.<sup>[15,17]</sup>

The solid-state structure of cluster **2** was determined on the  $[\text{Ph}_4\text{P}]\textbf{2}$  salt. The anion is shown in Figure 2, selected structural parameters are listed in Table S4 of the Supporting Information.

Also in this case, six metal atoms define an octahedron, centered by the interstitial nitride. The gold atom is situated on the triangular face composed of Mo, Co1 and Co4. The Co and Mo atoms bind differently to the gold atom. As in **1**, the Mo–N, Mo–CO and Mo–Co distances are longer by about 0.2 Å than the corresponding cobalt bonds, whereas the difference between Mo–Au and Co–Au is almost 0.5 Å. The different abilities of the two metals to coordinate gold can probably be explained by their electronic configuration: the Mo atom, already depleted of electron density, is less prone to adding the electrophilic fragment than the Co atom. The addition of the Au–PPh<sub>3</sub> moiety brings about little change to the average structural parameters, but several distortions on the individual values, which can be related to electronic rather than to steric factors. As a matter of fact, the Co1–Co4 edge becomes abnormally long (2.810 Å), suggesting some reduction in its electron density. To compensate, N–Co1 and N–Co4 bonds are shortened, whereas Mo–N is lengthened, in contrast to the expected effect between the N(–3) donor and the Au(+1) acceptor. Also in **2**, no convincing conclusions can be drawn on the strength of Co–N and Mo–N interactions, since the difference in metallic radii, estimated from

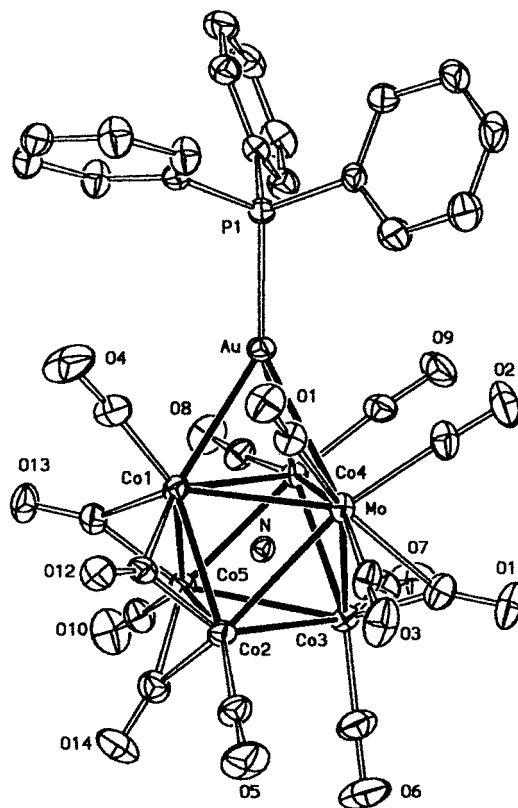


Figure 2. The solid-state structure of  $[\text{Co}_5\text{MoN}(\text{CO})_{14}\{\text{AuPPh}_3\}]^-$ ; carbon atoms are labeled using the oxygen atom to which they are attached

metal–metal and metal–nitrogen bond lengths, is even smaller than in **1** ( $0.07 \pm 0.10$  Å).

A very small lengthening of the M–CO (comparable, however, with uncertainties) might be indicative of reduced back-donation. The architecture of the bridging ligands is modified in **2**, and a “true”  $\mu$ -CO group, spanning a Co–Mo edge, is formed. The other three bridging carbonyl groups are located on the edges of the Co1, Co2, Co5 cluster face, which has the shortest Co–Co bonds. Thus, the shortening effect of the bridging ligands can also be observed in **2**.

### Electrochemistry and Joint EPR Measurements

Figure 3 illustrates the cyclic voltammetric behavior of  $[\text{Co}_5\text{MoN}(\text{CO})_{14}]^{2-}$  in MeCN solution.

Three sequential reductions with features of chemical reversibility are clearly detected together with an irreversible process interposed between the second and the third step. Taking into account that this latter process occurs at the same potential than that of an authentic sample of  $[\text{Ph}_4\text{P}]\text{Br}$ , we assign it to the counteraction of the cluster dianion.

Controlled potential coulometry corresponding to the first reduction ( $E_w = -1.5$  V) consumed one electron per molecule. In order to confirm the long-term chemical reversibility of such a process, cyclic voltammetry was performed on the exhaustively reduced solution, affording pro-

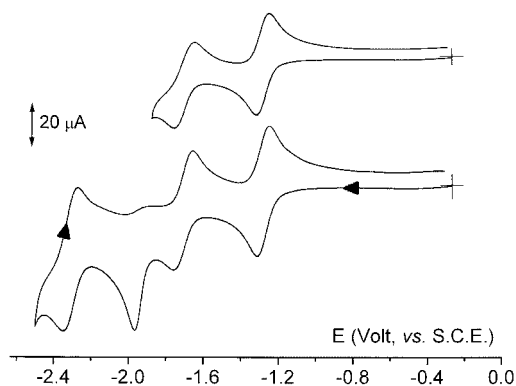


Figure 3. Cyclic voltammetric responses recorded at a gold electrode in an MeCN solution of  $[\text{Ph}_4\text{P}]_2[\text{Co}_5\text{MoN}(\text{CO})_{14}]$  ( $1.7 \times 10^{-3}$  mol·dm $^{-3}$ );  $[\text{Bu}_4\text{N}][\text{PF}_6]$  (0.2 mol·dm $^{-3}$ ); scan rate 0.2 V s $^{-1}$

files quite complementary to the original ones. On this basis we assign the series of chemically reversible reduction steps to the four-membered sequence  $[\text{Co}_5\text{MoN}(\text{CO})_{14}]^{2-/3-/4-/5-}$ .

Analysis of the  $[\text{Co}_5\text{MoN}(\text{CO})_{14}]^{2-/3-}$  process with scan rates increasing from 0.02 to 1.00 V s $^{-1}$  not only agrees with the chemical reversibility of the process ( $i_{\text{pa}}/i_{\text{pc}}$  constantly equal to unity), but also reveals its electrochemical reversibility ( $\Delta E_{\text{p}}$  constantly equal to 59 mV), thus suggesting that no significant geometrical reorganization accompanies the electron addition.<sup>[18]</sup>

The formal electrode potentials of the processes discussed above are compiled in Table 2. Finally, we point out that  $[\text{Co}_5\text{MoN}(\text{CO})_{14}]^{2-}$  also exhibits an irreversible multielectron oxidation ( $E_{\text{p}} = +0.13$  V).

In view of the chemical stability of the trianion  $[\text{Co}_5\text{MoN}(\text{CO})_{14}]^{3-}$ , EPR investigations have been carried out on the complex after its electrogeneration at  $-20$  °C. Figure 4 shows the X-band EPR spectrum of the MeCN solution of the trianion recorded under glassy conditions ( $T = 100$  K).

Table 2. Formal electrode potentials [V, vs. SCE] and peak-to-peak separations [mV] for the redox processes exhibited by  $[\text{Co}_5\text{MoN}(\text{CO})_{14}]^{2-}$  in MeCN solution

$E^{\circ'}_{(2-/3-)}$	$\Delta E_{\text{p}}^{[\text{a}]}$	$E^{\circ'}_{(3-/4-)}$	$\Delta E_{\text{p}}^{[\text{a}]}$	$E^{\circ'}_{(4-/5-)}$	$\Delta E_{\text{p}}^{[\text{a}]}$	$E_{\text{p}}^{[\text{a}][\text{b}]}$
-1.28	59	-1.70	85	-2.31	65	-1.97

[a] Measured at 0.2 V s $^{-1}$ . [b] Process centered on  $[\text{PPh}_4]^+$ , see text.

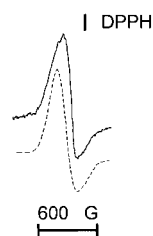


Figure 4. X-band EPR spectra of the frozen solution of  $[\text{Co}_5\text{MoN}(\text{CO})_{14}]^{3-}$ ;  $T = 100$  K; MeCN solution; solid line: first derivative experimental spectrum; dashed line: simulated spectrum

The lineshape analysis is suitably carried out assuming an  $S = 1/2$  axial electron spin hamiltonian with poor resolution of the overall anisotropic signal, which is constituted by two absorptions overlapped in the intermediate field.<sup>[19]</sup> The computed<sup>[20]</sup>  $g_i$  anisotropic parameters display a noticeable metal character ( $g_{\perp} > g_{\parallel} > g_{\text{electron}} = 2.0023$ ):

$$g_{\parallel} = 1.985(8), g_{\perp} = 2.160(8); \langle g \rangle = 1/3(g_{\parallel} + 2g_{\perp}) = 2.102(8)$$

$$\Delta H_{\parallel} = 110(5) \text{ G}; \Delta H_{\perp} = 95(5) \text{ G}$$

Neither Co ( $^{59}\text{Co}$ :  $I = 7/2$ ; natural abundance = 100%) nor Mo ( $^{97}\text{Mo}$ ,  $^{99}\text{Mo}$ :  $I = 5/2$ ; natural abundance = 15.8 and 9.6%, respectively) hyperfine (hpf) or superhyperfine (shpf) splittings are detected, as a consequence of the noticeable anisotropic line widths largely overlapping the underlying metal magnetic couplings, if any, i.e.

$$\Delta H_{\parallel} = 110(5) \text{ G} \geq a_i(^{59}\text{Co}, ^{97,99}\text{Mo}, ^{14}\text{N});$$

$$\Delta H_{\perp} = 95(5) \text{ G} \geq a_i(^{59}\text{Co}, ^{97,99}\text{Mo}, ^{14}\text{N})$$

The actual paramagnetic features indicate the complete delocalization of the  $S = 1/2$  unpaired spin density onto the octahedral metal frame without any evidence for significant individual metal interaction. The fact that the interstitial nitride nucleus ( $^{14}\text{N}$ :  $I = 1$ ; natural abundance = 99.6%) does not exhibit resolved anisotropic splittings, confirms this.

Raising the temperature of the glassy-fluid transition phase ( $T = 227.5$  K) results in the axial signal disappearing and the paramagnetic solution becoming EPR-mute. Rapidly refreezing the fluid solution only partially recovers the original anisotropic signal, indicating chemical lability of the electrogenerated trianion in fluid solution under a non-inert gas.

## Conclusions

The synthesis of the new cluster  $[\text{Co}_5\text{MoN}(\text{CO})_{14}]^{2-}$  was pursued hoping that substitution or addition of nitrogen or sulfur donors would highlight the cooperativity of the two metals in the coordination of the ligands and the cleavage of C–N and C–S bonds.<sup>[3]</sup> Even if it does not react directly with these types of ligands, the formation of  $[\text{Co}_5\text{MoN}(\text{CO})_{14}\{\text{AuPPh}_3\}]^-$  shows that more ligands can be added to its metal cage, and that both metallic elements are important for activation and coordination of electrophiles. Moreover, in contrast with what has been found in related dimetallic compounds,<sup>[9]</sup> the solid-state structure of both clusters allows us to exclude a preference of the nitride for the Co or Mo atom. The redox reactivity of the anion was studied by electrochemical and ESR experiments, that may suggest an alternative way to achieve substitution, through Electron Chain Transfer Catalysis (ECTC).<sup>[21]</sup> Therefore, we feel that the isolation of this dimetallic cluster can be relevant for material sciences, since it can be used as a molecular precursor to provide dimetallic nitrides, which



are active catalysts for the HDN reactions and for ammonia synthesis.<sup>[22]</sup> Additionally, after the discovery of an interstitial  $\mu_6$ -N atom in the Fe–Mo cofactor of nitrogenase,<sup>[23]</sup> carbonyl-nitrido clusters will also play an important role in the field of bioinorganic chemistry and  $N_2$  activation, either as starting materials for synthetic studies,<sup>[24]</sup> or as reliable references for spectroscopy.<sup>[25]</sup>

## Experimental Section

**General:** All solvents were purified and dried by conventional methods and stored under nitrogen. All reactions were carried out under oxygen-free nitrogen using the Schlenk-tube technique.<sup>[26]</sup>  $K[Co_6N(CO)_{15}]$ ,<sup>[27]</sup>  $[Et_4N]_2[Mo_2(CO)_{10}]$ ,<sup>[28]</sup> were prepared by literature methods. Infrared spectra in solution were recorded with a Nicolet Avatar FT-IR spectrophotometer, using calcium fluoride cells previously purged with  $N_2$ . Elemental analyses were carried out by the staff of the Laboratorio di Analisi of the Dipartimento di Chimica Inorganica, Metallorganica e Analitica. The materials and apparatus for the electrochemistry and joint-EPR measurements have been described elsewhere.<sup>[29]</sup> All of the potential values were referenced to the saturated calomel electrode (SCE). Under the present experimental conditions, the one-electron oxidation of ferrocene occurs at +0.38 V.

**Synthesis of  $[Co_5MoN(CO)_{14}]^{2-}$  from  $[Co_6N(CO)_{15}]^-$  and  $[Mo_2(CO)_{10}]^{2-}$ :**  $K[Co_6N(CO)_{15}]$  (1.21 g; 1.47 mmol) and  $[Et_4N]_2[Mo_2(CO)_{10}]$  (0.58 g; 0.79 mmol) were dissolved in MeCN (70 mL) and refluxed, while monitoring by IR spectroscopy. After about 7 h, the starting materials were completely consumed, the solution was cooled to room temperature and filtered to eliminate the insoluble material. The solvent was removed in vacuo and the residue was dissolved with methanol. Addition of  $[Ph_4P]Br$  caused precipitation of microcrystalline  $[Ph_4P]_21$ , which was filtered off, washed with 2-propanol and dried. It was then dissolved in the minimum amount of THF, and the solution layered with 2-propanol. Crystals of the salt  $[Ph_4P]_21$  were obtained in 20% yield. IR (THF;  $cm^{-1}$ ):  $\nu(CO) = 2019$  w, 1960 vs, 1832 m (see Figure S5 of the Supporting Information).  $C_{62}H_{40}Co_5MoNO_{14}P_2$  (1475.5): calcd. C 50.47, H 2.73, N 0.95; found C 50.24, H 2.15, N 0.85.

**Synthesis of  $[Co_5MoN(CO)_{14}\{AuPPh_3\}]^-$ :**  $[Ph_4P]_2[Co_5MoN(CO)_{14}]$  (0.10 g; 0.064 mmol) and  $Au(PPh_3)Cl$  (0.03 g; 0.062 mmol) were dissolved in THF (10 mL) and stirred at room temperature. After 15 min, the reaction was completed, the solvent was then removed in vacuo, and the solid was repeatedly washed with 2-propanol. It was then dissolved in a minimum amount of THF, and the solution was layered with 2-propanol. Yield 44 mg of  $[Ph_4P]_2$  (43%). IR (THF;  $cm^{-1}$ ):  $\nu(CO) = 2038$  m, 1986 vs, 1861 m, 1838 w in THF (see Figure S5 of the Supporting Information).  $C_{56}H_{35}AuCo_5MoNO_{14}P_2$  (1595.4): calcd. C 42.16, H 2.21, N 0.88; found C 42.08, H 1.86, N 0.85.  $^{31}P$  NMR ( $CD_2Cl_2$ ):  $\delta = 23.9$  ppm ( $[Ph_4P]^+$ ), 60.26 ppm ( $AuPPh_3$ ).

**X-ray Data Collections and Structure Determinations:** Crystal data are summarized in Table 3; for further experimental details see Supporting Information and ref.<sup>[14]</sup> The diffraction experiments were carried out with a Bruker SMART CCD area-detector diffractometer at 223 K. The collected frames were processed with the software SAINT,<sup>[30]</sup> and an empirical absorption correction was applied (SADABS)<sup>[31]</sup> to the collected reflections. The calculations were performed using the Personal Structure Determination Package<sup>[32]</sup> and the physical constants tabulated therein.<sup>[33]</sup> The structures were solved by direct methods (SHELXS)<sup>[34]</sup> and refined by full-matrix least squares using all reflections and minimizing the function  $\Sigma w(F_o^2 - kF_c^2)^2$  (refinement on  $F^2$ ). Anisotropic thermal factors were refined for all the non-hydrogen atoms. The hydrogen atoms were placed in their ideal positions ( $C-H = 0.97$  Å), with the thermal parameter  $B = 1.10$  times that of the carbon atom to which they are attached, and not refined. For noncentrosymmetric  $[Ph_4P]_21$  full refinement of the correct structure model led to  $R_2 = 0.064$  and  $R_{2w} = 0.090$ , full refinement of the inverted structure led to  $R_2 = 0.065$  and  $R_{2w} = 0.092$ . In the final Fourier maps the maximum residuals were  $1.87(15) e \cdot \text{\AA}^{-3}$  at  $0.78$  Å from Co(3) and  $0.92(18) e \cdot \text{\AA}^{-3}$  at  $0.89$  Å from Au for  $[Ph_4P]_21$  and  $[Ph_4P]_22$ , respectively.

**Supporting Information:** See footnote on the first page of this article.

## Acknowledgments

This work was financially supported by MIUR (cofin 2003 and FAR) and by Facoltà di Farmacia, Università di Milano.

Table 3. Crystallographic data and collection parameters for compounds  $[Ph_4P]_21$  and  $[Ph_4P]_22$

	$[Ph_4P]_21$	$[Ph_4P]_22$
Empirical formula	$C_{62}H_{40}Co_5MoNO_{14}P_2$	$C_{56}H_{35}AuCo_5MoNO_{14}P_2$
Formula mass	1475.56	1595.42
Crystal system	monoclinic	monoclinic
Space group	$Pc$	$P2_1/c$
$a$ [Å]	12.574(1)	11.828(1)
$b$ [Å]	13.242(1)	13.936(2)
$c$ [Å]	18.936(2)	35.084(4)
$\beta$ [°]	107.09(1)	94.89(1)
$V$ [Å <sup>3</sup> ]	3013.7(5)	5762(1)
$Z$	2	4
$T$ [K]	223	223
$\mu(Mo-K\alpha)$ [ $cm^{-1}$ ]	16.6	42.6
Reciprocal space explored	full sphere	full sphere
No. of reflections (total; independent)	50289, 18147	73246, 14505
$R_{int}$	0.033	0.038
Final $R_2$ and $R_{2w}$ indices ( $F^2$ , all reflections)	0.064, 0.090	0.046, 0.056
Conventional $R_1$ index $I > 2\sigma(I)$	0.038	0.027

- [1] R. Della Pergola, M. Branchini, A. Fumagalli, L. Garlaschelli, M. Manassero, M. Sansoni, *Eur. J. Inorg. Chem.* **2000**, 1759–1765.
- [2] T. Kabe, A. Ishihara, W. Qian, *Hydrodesulfurization and hydrodenitrogenation*, Wiley-VCH, Weinheim, **2000**.
- [3] [3a] R. J. Angelici, *Acc. Chem. Res.* **1988**, *21*, 387–394. [3b] C. Bianchini, A. Meli, *Acc. Chem. Res.* **1998**, *31*, 109–116. [3c] R. A. Sánchez-Delgado, *Organometallic Modeling of the Hydrodesulfurization and Hydrodenitrogenation Reactions*, Kluwer, Dordrecht, **2002**.
- [4] S.-I. Murahashi, Y. Imada, Y. Hirai, *Tetrahedron Lett.* **1987**, *28*, 77–80.
- [5] [5a] A. Eisenstadt, C. M. Giandomenico, M. F. Frederick, R. M. Laine, *Organometallics* **1985**, *4*, 2033–2039. [5b] M. Brorson, J. D. King, K. Kiriakidou, F. Prestopino, E. Nordlander, in *Metal Cluster in Chemistry* (Eds.: P. Braunstein, L. A. Oro, P. R. Raithby), Wiley-VCH, Weinheim, **1999**, vol. 2, p. 741–777. [5c] J. A. Cabeza, J. M. Fernández-Colinas, S. García-Granda, A. Llamares, F. López-Ortiz, V. Riera, J. F. Van der Maelen, *Organometallics* **1994**, *13*, 426–428.
- [6] M. D. Curtis, S. H. Drucker, *J. Am. Chem. Soc.* **1997**, *119*, 1027–1036.
- [7] M. D. Curtis, J. E. Penner-Hahn, J. Schwank, O. Baralt, D. J. McCabe, L. Thompson, G. Waldo, *Polyhedron* **1988**, *7*, 2411–2420.
- [8] Y. Okamoto, T. Kubota, *Cat. Surv. Jpn.* **2001**, *5*, 3–16.
- [9] C. P. Gibson, L. W. Dahl, *Organometallics* **1988**, *7*, 543–552.
- [10] The main IR band of **1** and that of Mo(CO)<sub>6</sub> overlap to a large extent.
- [11] K. Lee, J. R. Shapley, *Organometallics* **1998**, *17*, 4368–4373.
- [12] [12a] R. Della Pergola, L. Garlaschelli, M. Manassero, N. Masciocchi, *J. Organomet. Chem.* **1995**, *488*, 199–204. [12b] R. Della Pergola, A. Ceriotti, A. Cinquantini, F. Fabrizi de Biani, L. Garlaschelli, M. Manassero, R. Piacentini, M. Sansoni, P. Zanello, *Organometallics* **1998**, *17*, 802–806.
- [13] S. M. Waterman, N. T. Lucas, M. G. Humphrey, *Adv. Organomet. Chem.* **2001**, *46*, 47–143.
- [14] CCDC-230660 (for [Ph<sub>4</sub>P]<sub>2</sub>**1**) and -230661 (for [Ph<sub>4</sub>P]<sub>2</sub>**2**) contain the supplementary crystallographic data for this paper. These data can be obtained free of charge at [www.ccdc.cam.ac.uk/conts/retrieving.html](http://www.ccdc.cam.ac.uk/conts/retrieving.html) [or from the Cambridge Crystallographic Data Centre, 12 Union Road, Cambridge CB2 1EZ, UK; Fax: (internat.) + 44-1223-336-033; E-mail: [deposit@ccdc.cam.ac.uk](mailto:deposit@ccdc.cam.ac.uk)].
- [15] G. Ciani, S. Martinengo, *J. Organomet. Chem.* **1986**, *306*, C49–C52.
- [16] N. N. Greenwood, A. Earnshaw, *Chemistry of the Elements*, Pergamon Press, Oxford, **1989**, p. 480.
- [17] V. G. Albano, D. Braga, F. Grepioni, R. Della Pergola, L. Garlaschelli, A. Fumagalli, *J. Chem. Soc., Dalton Trans.* **1989**, 879–883.
- [18] P. Zanello, *Inorganic Electrochemistry. Theory, Practice and Application*, Royal Society of Chemistry, **2003**.
- [19] F. E. Mabbs, D. Collison, *Electron Paramagnetic Resonance of d Transition Metal Compounds*, Vol. 6 of the series *Studies in Inorganic Chemistry*, Elsevier, New York, **1992**.
- [20] P. Lozos, B. M. Hofmann, C. G. Franz, *Quantum Chemistry Program Exchange*, Indiana University, **1974**, 295, 20.
- [21] D. Astruc, *Angew. Chem. Int. Ed. Engl.* **1988**, *27*, 643.
- [22] [22a] S. Ramanathan, C. C. Yu, S. T. Oyama, *J. Catal.* **1998**, *173*, 10–16. [22b] P. Clark, B. Dhandapani, S. T. Oyama, *Appl. Catal. A: General* **1999**, *184*, L175–L180. [22c] V. Schwartz, S. T. Oyama, *J. Mol. Catal., A: Chem.* **2000**, *163*, 269–282.
- [23] O. Einsle, F. A. Tezcan, S. L. A. Andrade, B. Schmid, M. Yoshida, J. B. Howard, D. C. Rees, *Science* **2002**, *297*, 1696–1700.
- [24] S. C. Lee, R. H. Holm, *Chem. Rev.* **2004**, *104*, 1135–1157.
- [25] B. M. Leu, M. Z. Zgierski, G. R. A. Wyllie, W. R. Scheidt, W. Sturhahn, E. E. Alp, S. M. Durbin, J. Sage, *J. Am. Chem. Soc.* **2004**, *126*, 4211–4227.
- [26] D. F. Shriver, M. A. Dredzon, *The Manipulation of air-sensitive compounds*, 2nd ed., Wiley, New York, **1986**.
- [27] S. Martinengo, G. Ciani, A. Sironi, B. T. Heaton, J. Mason, *J. Am. Chem. Soc.* **1979**, *101*, 7095–7097.
- [28] J. K. Ruff, W. J. Schlientz, *Inorg. Synth.* **1974**, *15*, 88–90.
- [29] G. Ciani, A. Sironi, S. Martinengo, L. Garlaschelli, R. Della Pergola, P. Zanello, F. Laschi, N. Masciocchi, *Inorg. Chem.* **2001**, *40*, 3905–3911.
- [30] *SAINT Reference manual*, Siemens Energy and Automation, Madison, WI, **1994–1996**.
- [31] G. M. Sheldrick, *SADABS, Empirical Absorption Correction Program*, University of Göttingen, **1997**.
- [32] B. A. Frenz, *Comput. Phys.* **1988**, *2*, 42.
- [33] *Crystallographic Computing 5*, Oxford University Press, Oxford, U. K., **1991**, chapter 11, p. 126.
- [34] G. M. Sheldrick, *SHELXS 86, Program for the solution of crystal structures*, University of Göttingen, Germany, **1985**.

Received February 10, 2004

Early View Article

Published Online July 22, 2004